Fire Protective Surface Coating Containing Nanoparticles for Marine Composite Laminates

Léa Floch, Bianca da Cruz Chiochetta, Laurent Ferry, Didier Perrin, Patrick Ienny

Article

Fire Protective Surface Coating Containing Nanoparticles for Marine Composite Laminates

Léa Floch [1], **Bianca Da Cruz Chiochetta** [1], **Laurent Ferry** [1,*], **Didier Perrin** [1] and **Patrick Ienny** [2]

[1] Polymers Composites and Hybrids (PCH)—IMT Mines Ales, 30319 Ales, France; lea.floch@mines-ales.fr (L.F.); bianca.da-cruz-chiochetta@mines-ales.org (B.D.C.C.); didier.perrin@mines-ales.fr (D.P.)
[2] LMGC, IMT Mines Ales, University of Montpellier, CNRS, 75016 Paris, France; patrick.ienny@mines-ales.fr
* Correspondence: laurent.ferry@mines-ales.fr

Abstract: A poly(vinyl alcohol) (PVA)-based coating containing ammonium polyphosphate (APP) and sepiolite nanofillers (SP) and supported by a glass fabric was developed to fire-protect a glass-fiber-reinforced unsaturated-polyester-based (UP) polymer (GFRP). The fire behavior and thermal stability of the PVA coatings were characterized using thermogravimetric analysis (TGA) and a cone calorimeter. The coatings' residues were investigated by X-ray diffraction (XRD) and scanning electron microscopy (SEM). The results from the cone calorimeter showed that the addition of sepiolite significantly improves the flame retardancy of PVA/APP/SP coatings. The addition of both additives promoted the formation of a cohesive layer composed of a silico-phosphate structure resulting from the reactivity between APP and SP. The fire resistance of the composite laminate protected by PVA coatings was evaluated using a cone calorimeter by measuring the temperature of the back face. Photogrammetry was used to assess the swelling of residues after heat exposure. The interaction between APP and SP in PVA coating leads to the formation of an effective thermal barrier layer. The presence of SP reduces the layer expansion but greatly decreases the backside temperature during the initial period of exposure. The effect was assigned to high thermal stability of the layer and its ability to dissipate heat by re-radiation.

Keywords: composite laminates; surface coating; fire resistance; thermal insulation; PVA; fire retardants; sepiolite; ammonium polyphosphate

1. Introduction

Glass-fiber-reinforced polymer (GFRP) composites started to be used in shipbuilding in the 1970s. Their intrinsic properties such as corrosion prevention and good aging resistance in the marine environment make them ideal candidates to replace the traditionally used materials such as steels and aluminum alloys [1]. Indeed, corrosion of metallic structures generates high maintenance costs with long period of unavailability of equipment. The weight reduction achievable with composites is a significant advantage for lightening structures (over 10 wt% lighter for similar size of boat between aluminum and GFRP composite-vinylester-based [2]). However, the use of these materials in shipbuilding is accompanied by concern about their vulnerability to fire. The organic polymer matrix is responsible for the ignition and can release toxic gases during a fire [3]. Until 1994, the International Maritime Organization (IMO) in the SOLAS convention (International Convention for the Safety of Life at Sea) excluded the possibility of using combustible materials (including GFRP) for ship construction. This convention specifies minimum standards for the construction, equipment and operation of passenger ships operating in international waters. It is applied to ships carrying passengers and merchandises over 500 gross tonnage navigating in international waters. Chapter II-2 of this convention, added on 1 July 2002, describes that unconventional materials used in ships must be "fire restricting", meaning low release of heat and smoke and must not spread a fire to adjacent compartments. Test methods relating to fire reaction and fire resistance requirements are

described in the document. It is specified that the fire safety design may deviate from the descriptive requirements provided that the design meets the fire safety objectives. Consequently, alternative solutions including GFRP materials for the construction of ship bulkheads must be proposed. Presently, a combustible wall can be found in ships as long as it is coated with a 100 mm of rock wool cladding considered as incombustible. This cladding constitutes a loss of space and a significant gain in weight. To limit the loss of space, it is necessary to develop intrinsically fire-resistant composite materials to meet regulatory requirements.

GFRP used in most marine applications consists of glass fabrics as reinforcement and generally polyester or vinylester resin as the matrix. The case of unsaturated polyester resin (UP) has been more particularly investigated. Cured UP resins rapidly thermally degrade at temperatures above 300 °C to give volatile products (initially styrene) that are easily ignited and burn with smoke [3]. There are several flame-retardant (FR) solutions that can improve the flame retardancy of GFRP. A first way consists of modifying the resin by using comonomers with a flame-retardant action. Kandola et al. used modified novolac [4] but also phenolic resoles [5] cured with UP with styrene as a reactive diluent. The resulting resin exhibited better flame retardance than pure UP. Tibiletti et al. synthesized a phosphonated styrenic comonomer that can partially substitute the reactive diluent in UP. This comonomer led to the creation of an efficient char layer during combustion [6]. A second way consists of incorporating FR additives into the polyester matrix. Interesting results have been obtained by combining classical FR with nanoparticles. Kandare et al. investigated the thermal behavior of flame-retarded UP containing ammonium polyphosphate (APP), zinc borate and organo-modified montmorillonite. An increase of the thermal stability as well as the char yield was observed [7]. Tibiletti et al. studied an FR system composed of alumina trihydrate (ATH) and alumina nanoparticle. Synergistic effects were highlighted on the thermal stability and heat release rate that were attributed to size complementarity between micro- and nanoparticles [8]. Most of the time, the improvement of composite fire properties comes with a reduction in the mechanical strength, which is detrimental for the lifespan of a ship [3,9]. A third possible way to improve the fire resistance of GFRP without changing the intrinsic properties of the material is the use of flame-retardant coatings [3,10]. The structural integrity of a composite wall can be maintained if the flame-retardant coating acts as a thermal barrier to protect the matrix from an increase in temperature due to a flame. Several studies have shown that ceramic [11] or intumescent coatings [5] are the most effective in forming a thermal barrier to limit the propagation of heat into the materials [10,12]. The result of the intumescence process is the swelling and growth of a char layer that insulates the material from the action of a heat source or a flame [13].

Poly(vinyl alcohol) (PVA) is a film-forming polymer used in several applications as packaging films, coatings, adhesives and biomaterials because of its good chemical resistance and moisture and oxygen barrier protection [14]. In addition, PVA is a biodegradable and nontoxic polymer, easy to process with a relatively low production cost. As regards to the fire properties, PVA is highly flammable (LOI = 19%) [15]. However, as a polyol polymer, it exhibits intrinsic charring properties that make it a good candidate as a charring agent in intumescent systems when combined with appropriate flame retardants. Several studies have shown the effectiveness of intumescent systems based on ammonium polyphosphate (APP) in the PVA matrix [15,16]. The authors investigated the morphology of residues of PVA/APP after a cone calorimeter or LOI (limited oxygen index) test. A swollen and compact structure was observed by SEM which appeared to provide a good barrier to the transfer of heat, mass and flammable gases during a fire. APP has been reported to mainly play a role in the condensed phase [15,17]. In the presence of a heat source, APP decomposes into polyphosphoric acid and promotes a dehydroxylation process in decomposing oxygen-containing polymers. Polyaromatic structures form and lead to a residual char which constitutes a protective layer at the surface of the decomposing material isolating the non-degraded polymer from the flame. However, an intumescent sys-

tem with APP alone requires a high charge rate (typically greater than 30 wt%) to achieve good fire performance [18]. In addition, the presence of a high level of flame retardant in a polymer matrix tends to result in a loss of mechanical properties. Nanoparticles have been incorporated into polymers because they are likely to improve mechanical performance as well as thermal stability and fire resistance for low loading rates [17,19,20]. Moreover, it has been shown that nanoparticles can be used in intumescent FR systems in order to improve the mechanical strength of the expanded char layer [21]. Sepiolite is a magnesium silicate clay material with the theoretical formula $(Si_{12}Mg_8O_{30})(OH_4)(OH_2)_4.8H_2O$ with H_2O representing zeolitic water present in an intra-crystalline cavity (tunnel). Sepiolite is characterized by blocks of octahedral sheets of magnesium oxides and hydroxides between two tetrahedral silica layers. In each tunnel, the octahedral sheets are bound with two H_2O molecules which correspond to coordinated water and are weakly bound with zeolitic water [22]. Sepiolite exhibits a needle morphology which generates a high specific surface area of 200–300 m^2/g, lengths of 0.2–4 µm and a width of 10–30 nm and thickness of 5–10 nm [23]. It is a hydrophilic nanoparticle—it can be added into PVA matrix by simply dispersing in water [14]. However, only a few works have reported the use of sepiolite in flame-retardant systems in combination with APP [24–26]. Vahabi et al. [24] investigated the thermal behavior and flame retardancy of poly(methyl methacrylate) containing APP (Exolit AP422) and sepiolite (Pangel S9). The authors reported a decrease of 65% of the peak of heat release rate (pHRR) and an increase of 29 wt% of the residue with respect to the virgin matrix after cone calorimeter tests. The presence of sepiolite particles make the residue more compact and less porous which leads to an improved barrier effect of the residue during combustion. Pappalardo et al. [25] reported in a propylene matrix a considerable decrease of the pHRR by 80% during cone calorimeter tests with the incorporation in an extruder of an APP (Exolit AP 766) and sepiolite (Sigma Aldrich). Carretier et al. [26] investigated polyurethane/APP (Exolit AP423)/Sepiolite (Pangel S9) ternary systems prepared by casting in a mold at 155 °C and observed that the pHRR decreased by 88% and the residue increased by 17 wt%. The authors suggested the interest of choosing a ratio of 3 between APP and sepiolite allowing the presence of free sepiolite which could play an additional thermal barrier effect.

This work aims at assessing the effectiveness of sepiolite and APP as fire retardant agents in PVA for the manufacture of a surface coating containing nanoparticles to protect GFRP composites during a fire with the objective to improve both the reaction-to-fire and the thermal insulation. The influence of APP content in the PVA matrix was firstly studied for a rate of 10 to 40 wt%. Then APP/sepiolite mixtures were investigated at a fixed loading rate of 20 wt% in PVA. The substitution of a high rate of APP loading by sepiolite was carried out in order to investigate the impact on fire properties for an acceptable loading rate in terms of mechanical property. This study focuses on the mechanisms of fire retardancy induced by the presence of both additives in PVA as well as their influence on fire reaction and fire resistance of coatings designed to protect GFRP composites. Fire reaction and fire resistance were assessed at the macroscopic scale using cone calorimeter and surface temperature measurements. Moreover, investigations on cone calorimeter residues from coatings and coated composite laminates were carried out. XRD analyses, SEM observations and thermogravimetric analysis were achieved to account for the interactions occurring between the various components during thermal degradation.

2. Material and Methods

2.1. Materials

The Poly (vinyl alcohol) (Selvol grade 203 s) was supplied by Sekisui company (Osaka, Japan). PVA was partially hydrolyzed with an average alcoholysis degree of 87–89% (M_w = 13,000–23,000). Ammonium polyphosphate (Exolit AP423) was obtained from Clariant (Muttenz, Switzerland). AP423 particles exhibit a 2 µm to 13 µm average diameter [17] and an average particle size (D50) of 8 µm. Sepiolite (Pangel S9 (SP)) was provided by Tolsa Company (Madrid, Spain).

Orthophthalic-based unsaturated polyester (commercial name Synolite 8488 G-2) is a pre-accelerated resin with a styrene content of 35 wt% in solution in dicyclopentadiene (DCPD) and was sourced by DSM Composites Resins. Methyl ethyl ketone peroxide (MEKP)-based catalyst (2%) in dimethyl phthalate for curing the resin was sourced from Akzo Nobel. Biaxial E glass-fiber fabric (0°/90°) with weight of 600 g/m^2 used as reinforcement was provided by Formax.

2.2. Sample Preparation

PVA suspensions were prepared according to the following process. First, APP and SP powders were mixed with mechanical stirring for about 10 min to break the long fibers of the sepiolite. PVA aqueous solution (35 wt%) was obtained by dissolving polymer into deionized water at 85 °C for 30 min. Then, flame-retardant powders were added to the PVA solution with mechanical stirring for about 30 min. The resulting suspensions were used to prepare either coatings or a fabric-based coating. The former was used to characterize the intrinsic properties of PVA/APP/sepiolite films; the latter was used to manufacture coated composite laminates.

For coatings, the PVA suspension was poured onto a glass plate coated with Teflon to form a sheet of 100 × 100 × 2.8 ± 0.03 mm. Fabric-based coatings were prepared by pouring the PVA suspension onto an E-glass fabric. The plate was dried at 45 °C for 24 h on a hot plate. The total content of APP and SP in PVA was kept constant at 20 wt%. Sepiolite was added with mass fractions of 1, 3 and 5 wt%. The sample names are listed in Table 1.

Table 1. Formulation of poly(vinyl alcohol) (PVA) coatings containing ammonium polyphosphate (APP) and Sepiolite with 20 wt% total loading in flame retardant.

Nomenclature	Component (wt%)		
	PVA	APP	Sepiolite
PVA	100	0	0
PVA/APP10	90	10	0
PVA/APP20	80	20	0
PVA/APP30	70	30	0
PVA/APP40	60	40	0
PVA/APP19/SP1	80	19	1
PVA/APP17/SP3	80	17	3
PVA/APP15/SP5	80	15	5

For fire resistance tests, glass-fiber reinforced composites (hereafter referred to as composite laminate) were fabricated by infusion in the form of sheets of 250 × 220 × 3.7 mm^3. Composite laminates were prepared with eight plies of 250 mm × 220 mm woven E-glass fabric (600 g/m^2), with a typical ratio of 68 wt% glass fiber and 32 wt% resin matrix. For coated composite laminates, the fabric-based PVA coating was placed on Teflon plate and eight glass fiber plies were added on top.

Then composite laminate was obtained by a vacuum infusion process and curing at room temperature for 24 h. The structure of coated composite laminates is shown in the Figure 1. The GFRP composites were further cut in 100 × 100 × 7.1 ± 0.4 mm for fire tests. A good cohesion between surface coating and composite laminate was observed by optical microscopy as illustrated in Supplementary Materials.
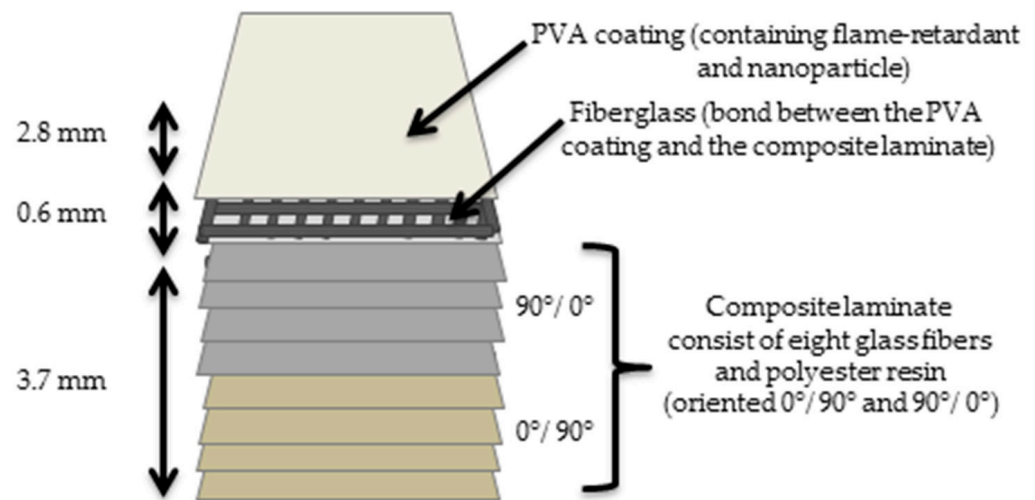
Figure 1. Schematic illustration of the arrangement of PVA coating complex on the composite laminate.

2.3. Characterization

2.3.1. Thermogravimetric Analysis (TGA)

Thermogravimetric analysis (TGA) was performed on a Setaram instrument Setsys TGA thermogravimetric analyzer in alumina crucibles containing around 10 ± 1 mg of material ranging from 30 °C to 900 °C with a heating ramp of 10 °C. min^{-1} under a nitrogen atmosphere.

2.3.2. Cone Calorimeter

Cone calorimeter tests were performed on a fire testing technology (FTT) apparatus to study the fire reaction of the PVA/APP/SP coatings according to ISO 5660. Samples (100 mm × 100 mm × 2. 8 ± 0.3 mm) were placed horizontally onto a balance and exposed to a 50 kW/m^2 heat flux in air under well-ventilated conditions (air flow rate 24 L/s). Tests were carried out with a piloted ignition. The results focused on time to ignition (TTI), heat release rate (HRR) curves, peak of HRR (peak HRR) and total heat release (HRR). The results presented in this study correspond to the mean values obtained from three experiments for each formulation. For each a standard deviation of around 10% was observed. Char residues obtained after cone calorimeter tests were examined by scanning electron microscopy (SEM) and X-ray diffraction (XRD).

A cone calorimeter was also used to assess the fire resistance of GFRP plates and GFRP protected by the following coatings: PVA, PVA/APP20, PVA/APP17/SP3 and PVA/APP15/SP5. In order to evaluate the coating efficiency in both flaming and non-flaming conditions, the coated plates were submitted to irradiances of 20 kW/m^2 and 50 kW/m^2. Heat flux of 20 kW/m^2 was set to provoke thermal decomposition without ignition. Conversely, heat flux of 50 kW/m^2 was supposed to lead to flaming conditions based on the results of coating fire reaction. The cone calorimeter was put in a vertical position (distance of 25 mm) without forced ignition and the temperatures of the backside were measured in the middle of the plate using an Optris® CT laser pyrometer.

2.3.3. Scanning Electron Microscopy (SEM)

Images of the cross-sections of the PVA coating were obtained with a SEM microscope (FEI Quanta 200F) using a secondary electron imaging. All observations were achieved under high vacuum at a voltage of 3.0–12.5 kV with a spot size of 3 mm and a working distance of 8–10.4 mm. PVA coatings were observed after fracture in liquid nitrogen followed by carbon deposition to make the material conductive. Residues of PVA coatings after fire reaction tests were observed without any preparation. Energy dispersive X-ray

spectroscopy (EDX) was performed with the same device to acquire information about residues' surface composition and after grinding and mixing residues of PVA coatings.

2.3.4. XRD Analysis

XRD patterns were obtained on a Bruker AXS D8 Advance X-ray powder diffractometer using the Cu Kα radiation. The residue powders were dried at 80 °C for 12 h under vacuum, crushed and compacted with a glass slide for analysis. Residues of PVA coatings after fire reaction and fire resistance tests were analyzed. In order to assess the reactivity between APP and sepiolite, blends of PVA/APP/SP and APP/SP were heated in an oven at three temperatures chosen in view of the TGA results (200 °C, 350 °C and 550 °C) for 3 h. Compacted powder pellets of about one gram of materials were placed in the oven. After treatment, the partially degraded materials were characterized by XRD.

2.3.5. Photogrammetry

Photogrammetry was performed to estimate the volume of cone calorimeter residues. A camera Canon EOS 7D, a rotational table and a fixed light were used to take pictures with steps of 10° (36 pictures), for two angles (30° and 45°). This resulted in the acquisition of 72 images in raw format, processed by the software Agisoft Metashape to generate the 3D objects. The grid was finally analyzed using the software Cloud Compare. A calibration factor α was determined to convert the size from pixels to centimeters. The computational volume was then calculated using the software, and finally, the real volume was calculated by multiplying the computational volume by α^3.

3. Results and Discussions

The results and discussions section is divided into subsections. Part 3.1 shows dispersion of particles in PVA coatings. Part 3.2 and 3.3 describe TGA and cone calorimeter results on the PVA coatings. Characterization by EDX and XRD of the residues after cone calorimeter test are also presented in Part 3.4. Fire efficiency of PVA coatings on GFRP composite laminate is evaluated in fire resistance with cone calorimeter tests in Section 3.5. SEM, XRD and photogrammetry of the residues of PVA coatings on composite laminate are shown.

3.1. Dispersion of Particles in PVA/APP/SP Coatings

An SEM picture of pure sepiolite is presented in Figure 2. The nanoparticle exhibits a fibrous morphology, as expected. The fiber diameter is lower than 100 nm while the fiber length may exceed 10 μm [27]. The state of dispersion in the PVA/APP/SP 3 wt% coating can be observed in Figure 3.
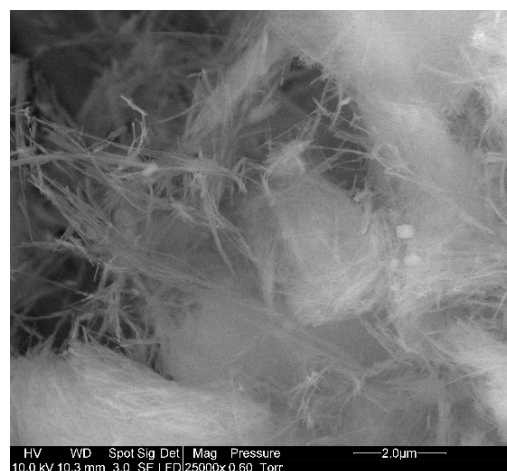

Figure 2. SEM picture of sepiolite (Pangel) for magnification of 25,000.
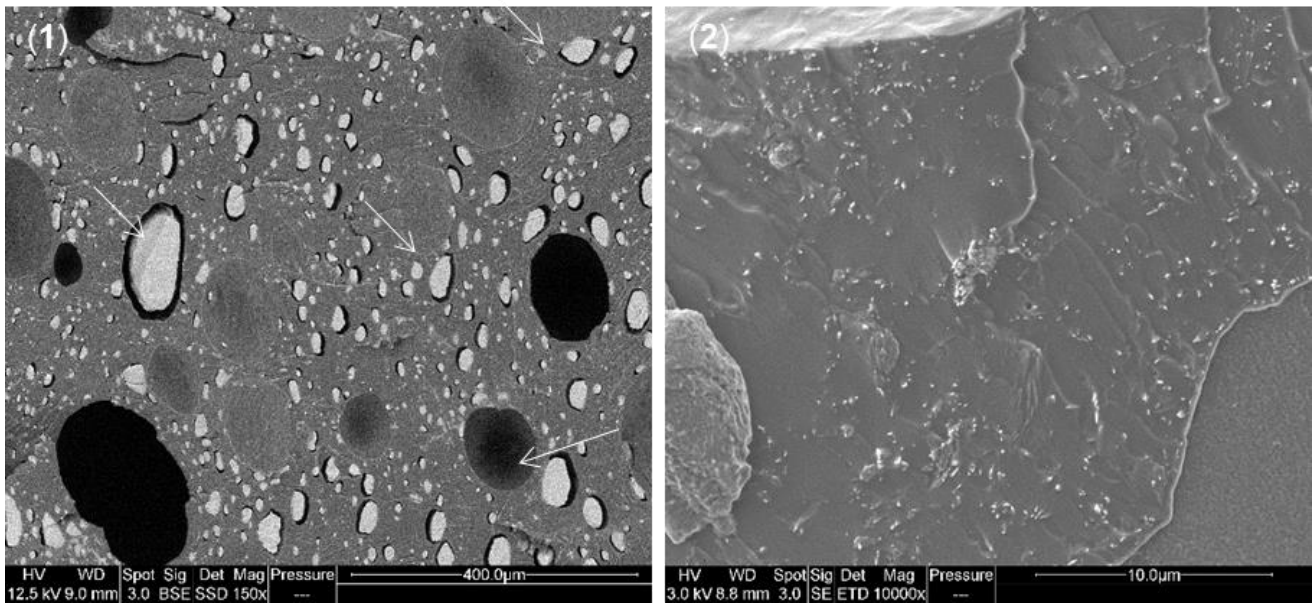
Figure 3. SEM pictures of PVA/APP/SP (SP 3 wt%) composite for magnification of 150 (1) and 10,000 (2) (aggregates of APP are shown by arrows). SP: sepiolite nanofillers.

Some aggregates of APP particles can be found with size ranging from 5 to 70 µm.

However, it seems that APP is homogeneously dispersed in the PVA matrix despite the formation of aggregates. In addition, poor adhesion with the PVA matrix is evidenced by the dark corona around the APP aggregates. The presence of a large porosity is observed due to air trapping during the drying process on the plate. Finally, a homogeneous dispersion of the sepiolite fibers within the matrix is observed on the SEM images on the surface of the material at a higher magnification.

3.2. Thermal Behavior of PVA Coatings

The thermal degradation of coatings was studied by TGA under N2 flow, and the resulting TGA and differential thermogravimetric (DTG) curves are presented in Figure 4 and Table 2. The initial decomposition temperature (T_{onset}) is defined as the onset temperature. As already observed in references [28,29], the thermal degradation of PVA is broken down in three steps. The first mass loss, at circa 100 °C, is attributed to evaporation of water physically bonded to hydroxyl groups of PVA. The main mass loss of the polymer occurs in the second step at circa 320 °C, characterized by the degradation of residual acetate groups and elimination of water [15]. Lastly, at circa 440 °C, the third and final step given is due to the degradation of unsaturated chain residues by chain-scission or cyclization reactions, leaving 2.34% of char yield at 900 °C. Additionally, the process of degradation of APP is carried out in three steps, in which the first two are due to release of water and ammonia leading to the formation of polyphosphoric acid [30] and the last step is due to phosphate chain fragmentations [31].
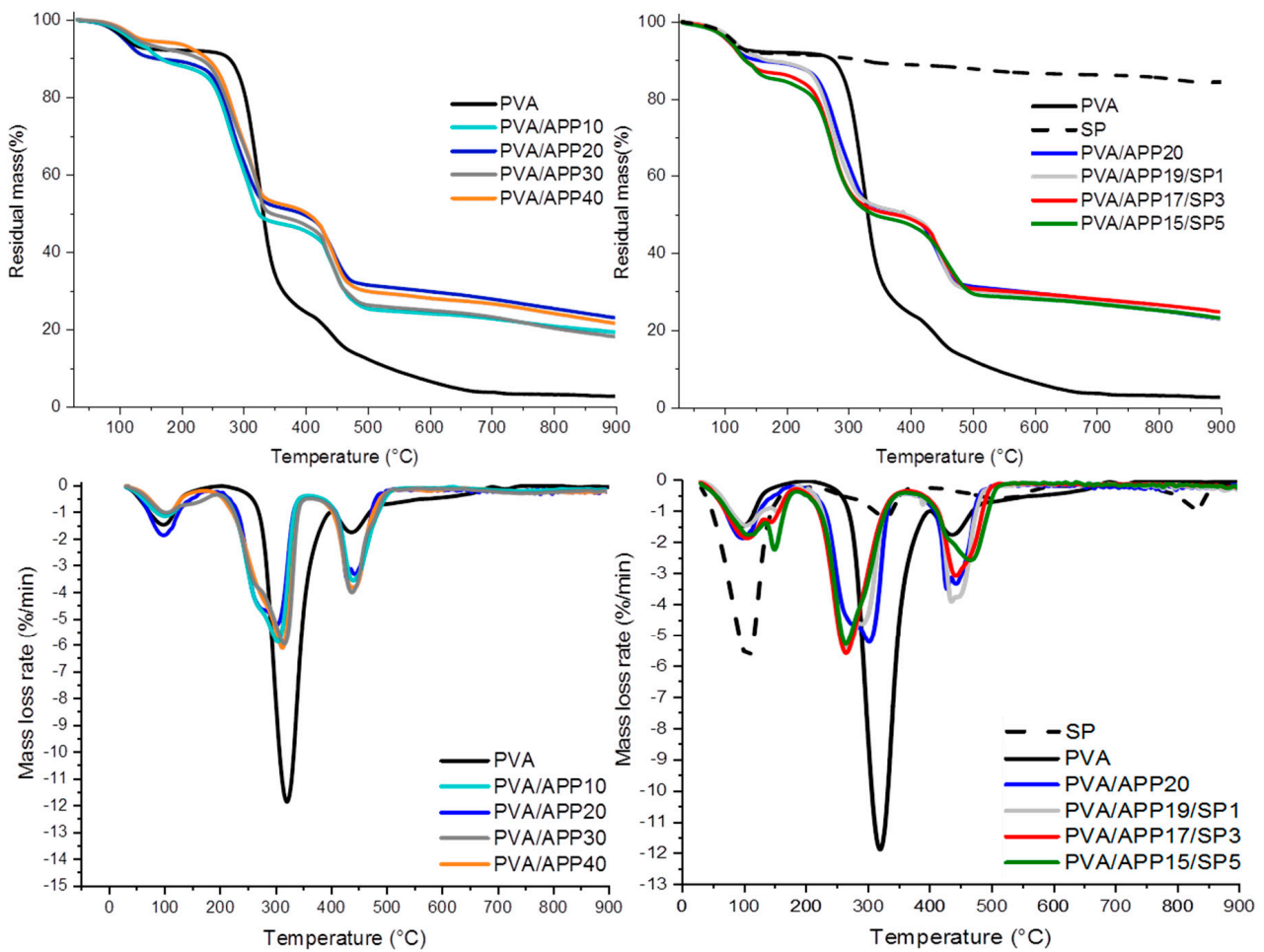
Figure 4. Thermogravimetric analysis (TGA) and differential thermogravimetric (DTG) of pure PVA and PVA coatings under N2.

Table 2. TGA data for PVA-based composites.

		Residue (%)		
Nomenclature	Tonset (°C)	700 °C (Exp$_{res}$)	Th$_{res}$	Exp$_{res}$–The$_{res}$
PVA	291	3.47	2.34	-
PVA/APP10	249	22.60	8.22	14.37
PVA/APP20	248	27.64	13.27	14.36
PVA/APP30	247	23.00	18.31	4.68
PVA/APP40	247	24.47	23.36	1.11
PVA/APP19/SP1	248	27.27	14.90	12.37
PVA/APP17/SP3	243	28.00	14.25	13.75
PVA/APP15/SP5	238	26.71	13.59	13.11

The addition of 20 wt% of APP to the PVA matrix induces decomposition at a lower temperature (248 °C), with a main step of degradation at 304 °C. The phosphoric acid resulting from the thermal degradation of APP leaves a viscous molten surface that protects the polymeric substrate, resulting in a dense char residue. The addition of APP to the matrix leads to the formation of approximately 20 wt% of char whatever the proportions of APP (in the range from 10 wt% to 40 wt%).

The thermal behavior of sepiolite fibers is presented in Figure 4. It was found that the crystalline structure of nanoclay is only affected at high temperature, undergoing hygroscopic, zeolitic and coordinated water loss up to 850 °C, after which, phase transfor-

mation to enstatite $Mg_2Si_2O_6$ takes place [14,32]. The behavior found in this paper is in agreement with the literature [32,33], where the sepiolite used in the coatings has its first step of degradation at 110 °C, representing the hygroscopic and zeolitic water loss. The second step at 330 °C represents the loss of about half of the coordinated water, followed by another step at 530 °C where the rest of the coordinated water is released. Finally, the last step at 840 °C corresponds to the formation of a crystalline structure of enstatite ($MgSiO_3$) by a dehydroxylation process leading to a loss of water [32].

The addition of sepiolite to the coatings seems to reduce the thermal stability that decreases from 248 °C for PVA/APP20 to 238 °C for PVA/APP15/SP5. Moreover, when the nanoclay content increases from 1 to 5 wt%, a slightly greater mass loss in the first step of decomposition is observed. This loss may be caused by the absorbed moisture and/or trapped water due to the interactions between PVA, water solvent and sepiolite [14]. There are no significant differences in char residue when sepiolite is added, which suggests that the char residue is mainly governed by APP. To conclude, thermal stability of PVA/APP/sepiolite coating is lower than that of pure PVA. The majority of this phenomenon is induced by the presence of APP but it seems that sepiolite has a slight impact on the thermal stability of the coating.

Theoretical residues of PVA coatings (The_{res}) have been calculated by a simple mixing law on the residue yield at 700 °C (1).

$$The_{res} = X_{PVA} \times PVA_{700} + X_{APP} \times APP_{700} + X_{SP} \times SP_{700}, \tag{1}$$

with X_{PVA}, X_{APP}, X_{SP} as the weight fractions of PVA, APP and SP. PVA_{700}, APP_{700}, SP_{700} are the experimental residue values at 700 °C.

Table 2 clearly shows that experimental residues at 700 °C are higher than the theoretical ones (Th_{res}) in PVA coatings. This result highlights the charring effect of APP upon PVA. The amount of char represents circa 12% to 14% of the initial mass for APP content up to 20 wt%. It has been observed that increasing the APP content above 20 wt% no longer increases the carbon yield.

3.3. Fire Behavior of PVA/APP/SP Coatings

To investigate the fire behavior of the PVA coatings, cone calorimeter tests were performed with a heat flux of 50 kW/m^2 which corresponds to a well-developed fire scenario. Heat release rate (HRR) curves are presented in Figure 5, and pHRR, THR, total smoke release (TSR), residue yield and time to ignition (TTI) data are presented in Table 3.
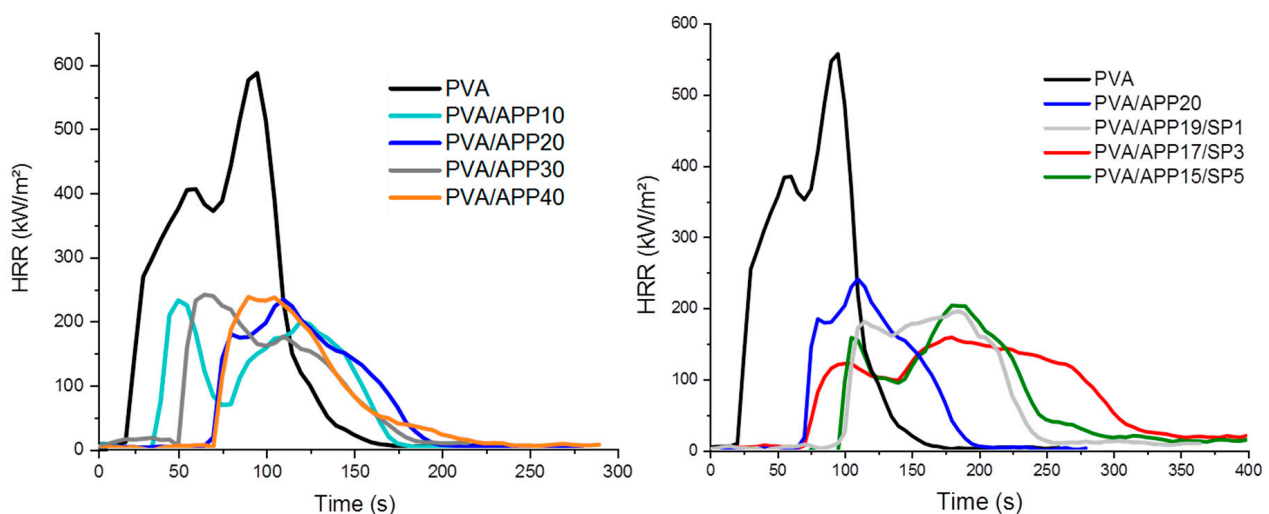

Figure 5. Heat release rate curves of PVA and PVA coatings on cone calorimeter for 50 kW/m^2.

Table 3. Cone calorimeter data for 50 kW/m^2 for PVA-based coatings.

Formulation	TTI (s)	pHRR (kW/m^2)	THR (MJ/m^2)	TSR (m^2/m^2)	Residue (%)
PVA	20 ± 2	558 ± 2	35 ± 1	334 ± 50	0
PVA/APP10	27 ± 14	242 ± 28	22 ± 1	757 ± 68	11.5 ± 2.0
PVA/APP20	81 ± 22	205 ± 39	19 ± 3	930 ± 89	17.6 ± 1.2
PVA/APP30	54 ± 8	254 ± 10	18 ± 1	890 ± 66	14.3 ± 0.2
PVA/APP40	72 ± 12	251 ± 36	14 ± 3	641 ± 70	22.9 ± 2.7
PVA/APP19/SP1	90 ± 13	193 ± 10	22 ± 2	1105 ± 24	15.6 ± 4.7
PVA/APP17/SP3	65 ± 25	158 ± 18	22 ± 6	1058 ± 109	16.5 ± 1.2
PVA/APP15/SP5	73 ± 28	208 ± 62	21 ± 6	1103 ± 81	15.2 ± 2.0

Cone calorimeter tests of PVA plates confirm that the polymer alone exhibits a low thermal stability and high flammability and ignitability. The shape of the HRR curve of the PVA plate indicates that its behavior is that of an intermediate thickness no charring sample [34], with a pHRR value of 558 kW/m^2. This type of curve is obtained for materials which do not undergo charring. The matrix itself has the lowest TTI and the presence of APP alters the degradation path resulting in increased ignition time. This phenomenon has already been observed in the literature [15]. When decomposing, APP forms polyphosphoric acid that may further react by phosphorylation with hydroxyl groups of PVA and play a role in the cohesion of the char residue. The formation of a surface layer may delay the inflammation of the material or limit the release of combustible gases. In TGA, it has been observed that the incorporation of APP into PVA decreases its thermal stability. However, the ignition time is increased. In fact, the PVA coatings during cone tests swell upon application of a heat flux, thus limiting the release of decomposition gases, which are at the origin of the ignition of the material. The addition of 20 wt% of APP reduces pHRR by 45% and THR by 54% and changes the behavior of the curve to that of a thick charring material [34]. This type of curve is obtained for materials characterized by an initial increase in HRR until an effective protective layer is formed. As the layer thickens, this leads to a decrease in HRR. The residue yield found after cone calorimeter testing (between 11 and 23 wt%) indicates that APP promotes the charring of the PVA matrix since these values are higher than the theoretical ones as calculated using Equation (1). This confirms the results observed in TGA, even if the char yield is lower than that determined at 700 °C.

The addition of sepiolite into the composite does not significantly change THR results and char yield. However, the presence of sepiolite has an influence on the pHRR. The pHRR of PVA/APP17/SP3 is reduced by 15% compared to PVA/APP20. The lowest values of pHRR were obtained for the combination between APP and nanoparticles. A percentage of 3 wt% of sepiolite corresponds to the optimum of performance for all fire-reaction parameters. These results indicate that the action of APP and sepiolite is mainly in the condensed phase through the formation of a char layer. This protective layer slows down the release of combustible gas delaying the ignition of the PVA coating and drastically reducing the pHRR. It should be noted that SP may have a negative impact on smoke production since a slight increase in the quantity of smoke released between PVA/APP and PVA/APP/SP compositions was noted.

3.4. Characterization of Cone Calorimeter Residues

3.4.1. Composition of the Char Residue by EDX Analysis

EDX analysis was achieved during SEM observations in order to quantify the presence of chemical elements in the residues. Measurements for each composite were carried out on the whole residue after grinding. Compositions of residues crushed after cone calorimeter is summarized in Table 4.

Table 4. Quantitative analysis by EDX of residues crushed after cone calorimeter.

Composition	%C	%O	%P	%Si	%Mg	%Na	% N	Residue after Cone Test (%)	%P_{ini} (%)	%P_{res} (%)
PVA/APP20	23.9	51.1	23.1	-	-	1.7	Not detected	17.6	6.3	4.0
PVA/APP19/SP1	30.1	47.8	19.2	0.6	0.5	1.4	Not detected	15.6	5.9	2.9
PVA/APP17/SP3	44.5	33.8	17.3	2.0	1.1	1.0	Not detected	16.5	5.3	2.8
PVA/APP15/SP5	41.4	37.8	14.0	3.6	1.8	0.9	Not detected	15.2	4.7	2.1

The main difference between the compositions of residues affects the carbon element rate. It seems that the presence of sepiolite induces an increase of the carbon content evidencing a charring effect. The percentages of silicon and magnesium show a small and non-significant variation. The presence of phosphorus in the residue decreases with the decrease of APP content. The EDX data make it possible to define whether the phosphorus is released in the gas phase or retained in the condensed phase. For that purpose, the phosphorus content initially presenting in the coating (%P_{ini}) (2) is compared to percentage of phosphorus remaining in the residue (%P_{res}) (3).

$$\%P_{ini} = (M_{phosphorous}/M_{APP}) \times (\%_{APP}), \tag{2}$$

$$\%P_{res} = (\%P_{EDX}) \times (\%_{residue}), \tag{3}$$

If the two percentages are equal then phosphorus remains in the condensed phase, while, if %P_{ini} is greater than %P_{res} then a part of phosphorus has been released into the gas phase during combustion. For all compositions %P_{res} is lower than %P_{ini} indicating that a non-negligible part of phosphorus is released into the gas phase during combustion. This result may be put in relation with the slight increase in the total amount of smoke released for the PVA/APP and PVA/APP/SP samples.

3.4.2. XRD Analysis of Residues

To understand the role of phosphorus in the residue, XRD tests were performed. At high temperature, the coating decomposes into char which oxidizes over time, only amorphous carbon and inorganic phases remain. The inorganic phases then play the role of a thermal barrier limiting the diffusion of heat throughout the material. The XRD patterns of PVA/APP/SP coating residues showing the inorganic phases created after the cone calorimeter tests are presented in Figure 6. It appears that PVA/APP20 leads to an amorphous structure after combustion. On the contrary, the presence of crystalline phases is clearly observed for the three compositions containing sepiolite.

It should be emphasized that the composition PVA/APP17/SP3 is the one exhibiting the highest number of diffraction peaks indicating a well-crystallized structure. It seems that the ratio 17:3 (APP: sepiolite) promotes the formation of a crystalline phase during combustion. In addition, the absence of the characteristic peak of sepiolite (for 2θ = 7.3°) indicates either that the proportion of nanoparticle is too low to be detected or that sepiolite has reacted with APP.

The use of X'pert High Score software did not allow the diffraction peaks to be attributed to a known crystalline species. However, in the literature [35], a similar pattern has been observed without identification for a mixture of poly (1,4-butanediol succinate) (PBS) containing 15 wt% of APP423 and 5 wt% of Algerian halloysite. From the chemical composition of halloysite [35], it can be assumed that the crystalline structure formed arises from an interaction between silicon, phosphorus and oxygen. Therefore, this phase will be noted SixPyOz hereafter.
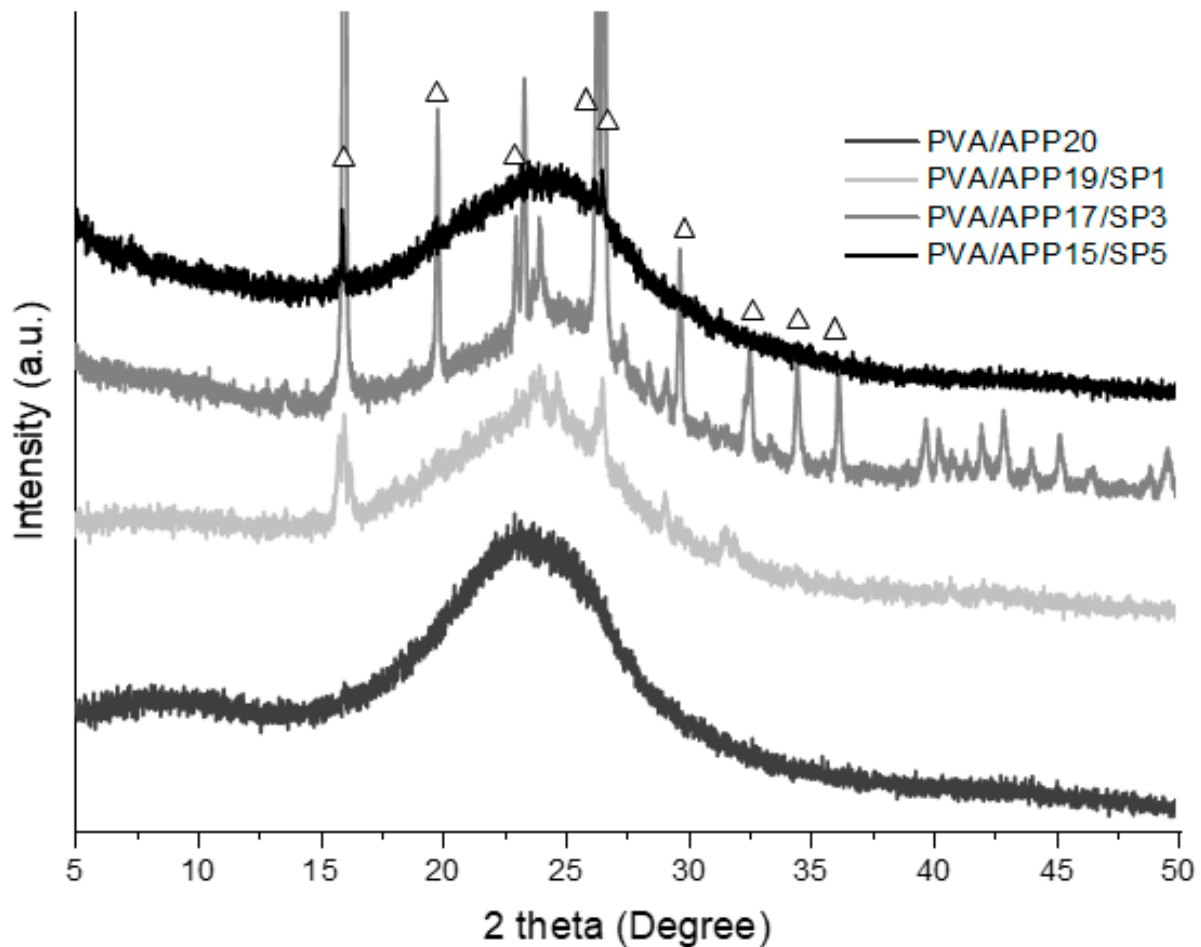
Figure 6. XRD patterns of PVA/APP/SP composites after fire reaction tests on a cone calorimeter at 50 kW/m² (($\triangle$): $Si_xP_yO_z$ phase).

To assess the reactivity between APP and sepiolite, sepiolite-containing coatings (PVA/APP17/SP3 and PVA/APP15/SP5) as well as sepiolite/APP blends (APP85/SP15 and APP75/SP25) were heated in an oven at three temperatures chosen in view of the TGA results (200 °C, 350 °C and 550 °C). These latter mixtures are representative of the proportions of sepiolite and APP in the compositions cited above.

The presence of sepiolite, sodium magnesium phosphate, ammonium magnesium phosphate, silicon phosphate and the $Si_xP_yO_z$ phase is shown by the XRD patterns (Figure 7) of PVA/APP17/SP3 and PVA/APP15/SP5 coating residues after oven conditioning. For PVA/APP17/SP3 at 350 °C and 550 °C, sodium magnesium phosphate and silicon phosphate crystals were identified through the presence of their main peaks (2θ = 23.3°, 25.0° and 35.6° for $NaMg(PO_3)_3$; 2θ = 24.0° and 26.3° for SiP_2O_7). For PVA/APP15/SP5 at 350 °C, ammonium magnesium phosphate was identified by peaks at 2θ = 15.8° and 17.2°. From 350 °C, APP is decomposed and creates an acid, which favors the reaction with sepiolite [24]. Sodium magnesium phosphate, ammonium magnesium phosphate and silicon phosphate are formed. At 550 °C, the $Si_xP_yO_z$ phase was characterized by peaks at 2θ = 16.0°, 19.8°, 26.3° and 26.5°. The absence of the crystalline phase SiP_2O_7 in PVA/APP15/SP5 sample was noted. This residue exhibited a less crystallized phase compared to the pattern of PVA/APP17/SP3 at 550 °C.
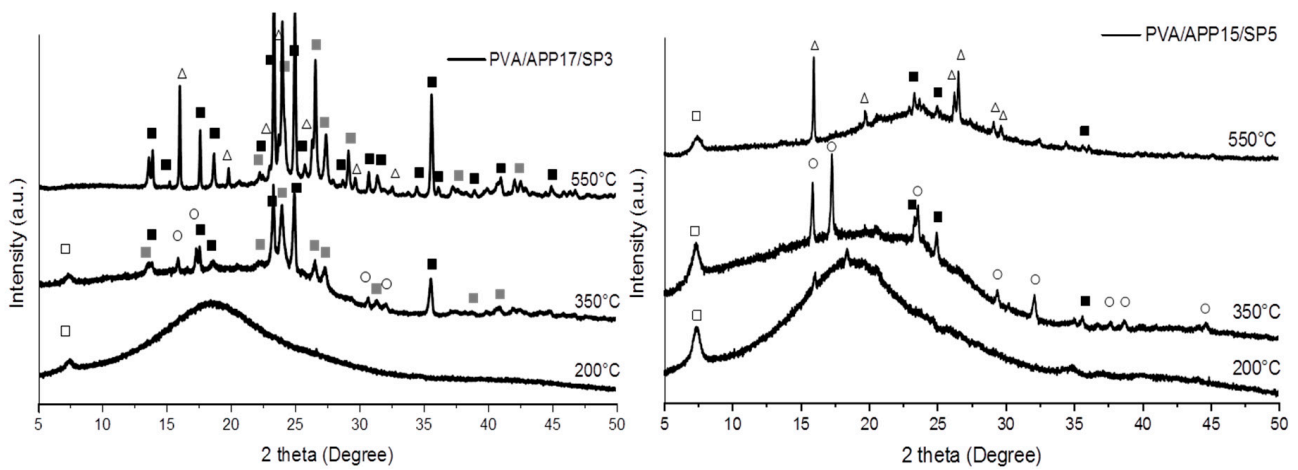
Figure 7. XRD patterns of PVA/APP17/SP3 and PVA/APP15/SP5 after oven conditioning at 200 °C, 350 °C and 550 °C (($\square$): sepiolite, ($\blacksquare$): $NaMg(PO_3)_3$, ($\blacksquare$): SiP_2O_7, ($\bigcirc$): $NH_4Mg(PO_3)_3$, ($\triangle$): $Si_xP_yO_z$ phase).

To verify reaction between SP and APP, XRD analyses were performed on mixtures APP/SP without PVA which were heated at 200, 350 and 550 °C. The XRD spectra of APP/SP powder mixtures are presented in Figure 8. At 200 °C, Sepiolite, ammonium phosphate ($NH_4(PO_3)$) and ammonium magnesium hydrogen phosphate hydrate (($NH_4)_2MgH_4(P_2O_7),2H_2O$) crystalline phases were observed for the two blends. Moreover, the presence of $NH_4Mg(PO_3)_3$ crystalline phase was noted at 350 °C. Ammonium phosphate, magnesium phosphate ($Mg_2P_4O_{12}$) and $Si_xP_yO_z$ phase crystalline phase were also formed at 550 °C whatever the APP/SP blending.
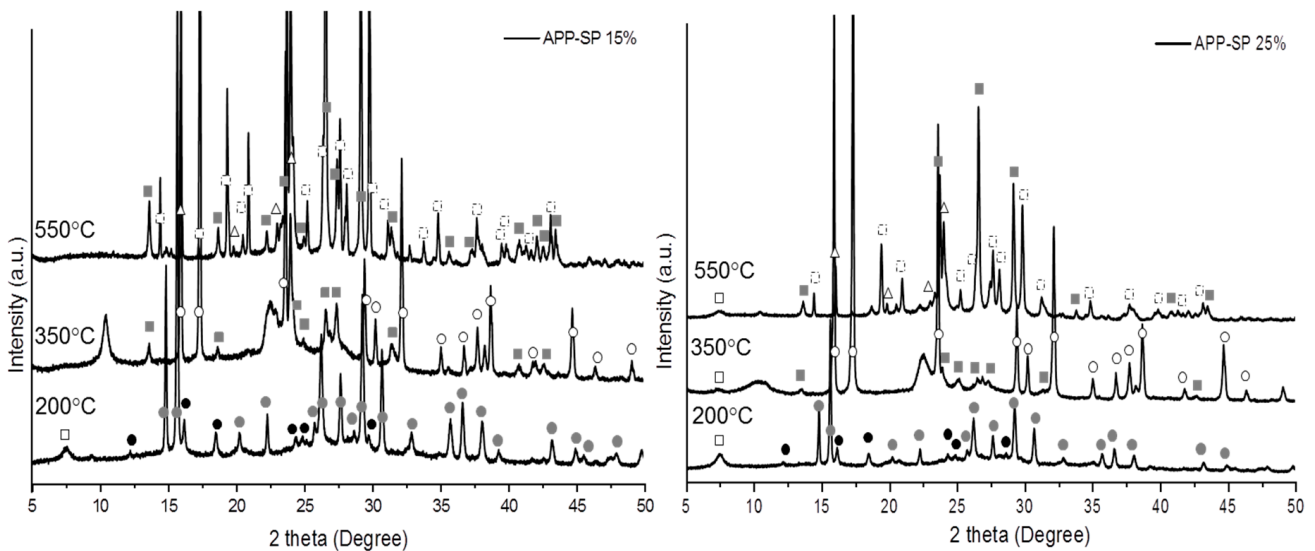

Figure 8. XRD patterns of APP/SP15 and APP/SP25 after oven conditioning at 200 °C, 350 °C and 550 °C (($\square$): sepiolite, ($\blacksquare$): SiP_2O_7, ($\bullet$): $(NH_4)_2MgH_4(P_2O_7),_2H_2O$, ($\boxdot$): $Mg_2P_4O_{12}$, ($\bigcirc$): $NH_4Mg(PO_3)_3$, ($\bullet$): $NH_4(PO_3)$, ($\triangle$): $Si_xP_yO_z$ phase).

However, in comparison with Figure 7, magnesium phosphate ($Mg_2P_4O_{12}$) and ammonium magnesium hydrogen phosphate hydrate ($(NH_4)_2MgH_4(P_2O_7),_2H_2O$) were not observed in the residue of PVA/APP/SP mixture. Therefore, XRD confirms the reaction between SP and APP at high temperature resulting in the formation of different crystalline phases such as $NH_4Mg(PO_3)_3$, SiP_2O_7 and $Si_xP_yO_z$ phase. Sepiolite crystalline phase was detected for all temperatures for PVA/APP15/SP5 and only at 200 °C and 350 °C for the PVA/APP17/SP3 sample. In this latter case, it can be assumed that a large proportion

of the sepiolite reacted with APP to form phosphorus-containing species. Based on the reaction between SP and APP and the results of Table 4, it can be concluded that the effect of APP in PVA/APP/SP coatings occurs in the condensed phase.

Oven tests demonstrated the APP-sepiolite interaction but all crystalline phases shown in Figure 6 were not found in cone calorimeter residues. It may be due to different temperatures and heating conditions between oven conditioning and the cone calorimeter test. However, the creation of the crystalline phase $Si_xP_yO_z$ phase seems to play a positive role in the flame-retardant action of this system during the cone calorimeter test.

3.4.3. Morphology of the Residues

Figure 9 shows the residues of coatings after the cone calorimeter tests highlight a difference depending on the presence of sepiolite. PVA gives no residue whereas the PVA/APP20 residue has swelled and appears thin and fragile. Conversely, for the other formulations, the residues are more cohesive with a thin and more resistant layer. It can be assumed that the development of this cohesive structure is capable of protecting the underlying polymer by limiting the propagation of the flame and the gas transfer. This layer could also limit the transmission of heat to the GFRP composite. To assess the efficiency of this structure, fire resistance tests were carried out using the calorimeter cone and will be presented in the following section.
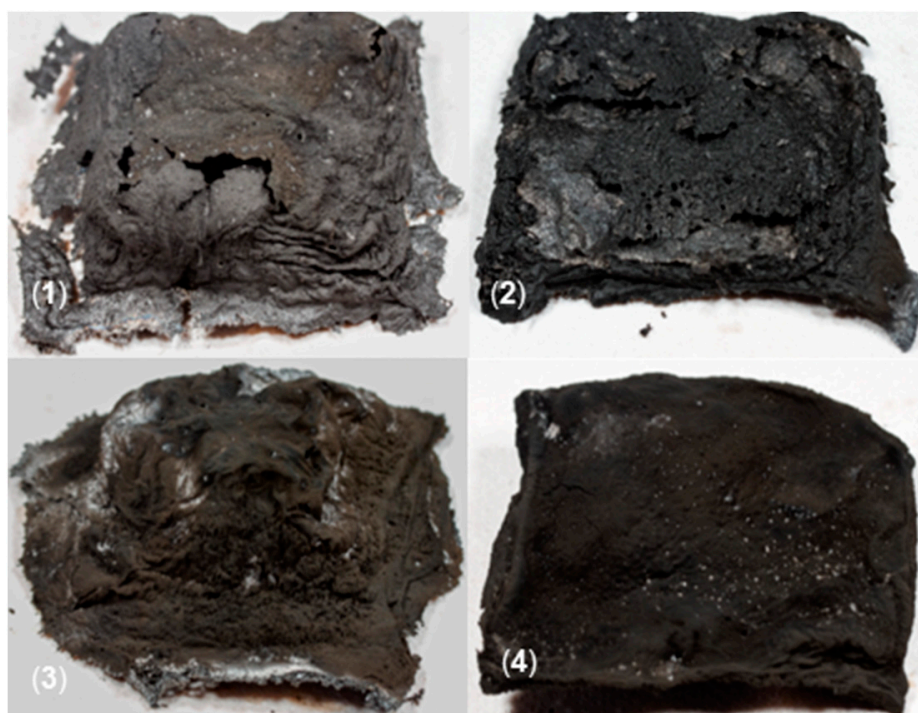

Figure 9. Photographs of char residues of PVA coatings after cone calorimeter experiments: (1) PVA/APP20, (2) PVA/APP19/SP1, (3) PVA/APP17/SP3, (4) PVA/APP15/SP5.

SEM was performed on residues after the cone calorimeter test to investigate their microstructure. The outer surfaces of the PVA/APP and PVA/APP/SP residues are shown in Figure 10.
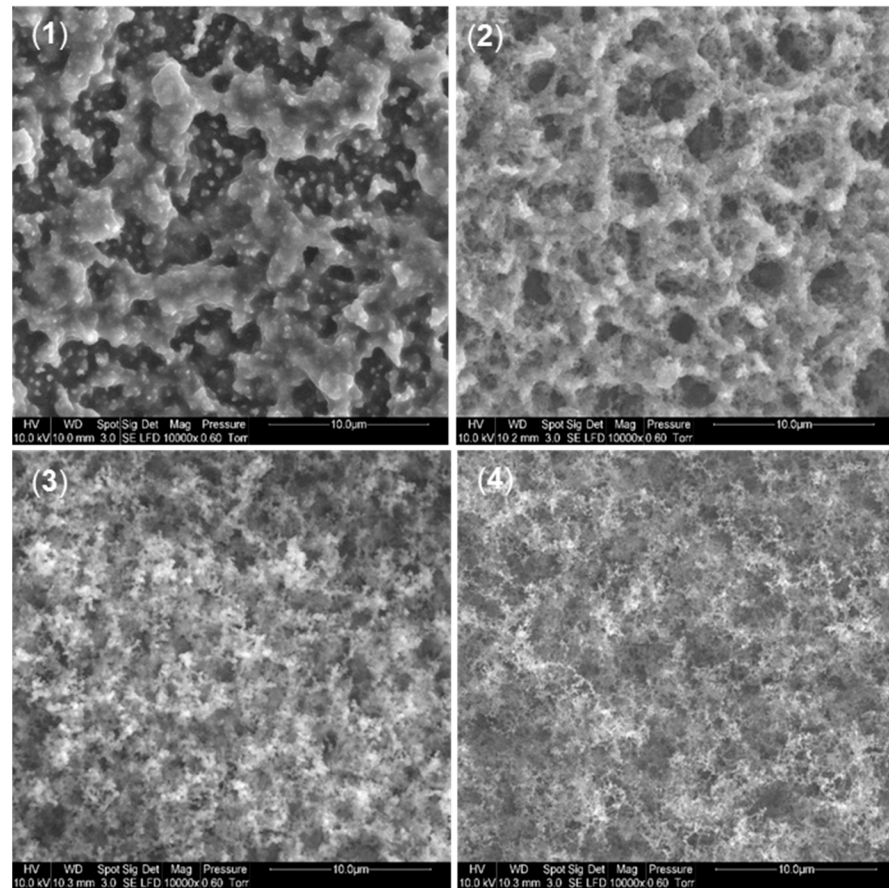
Figure 10. SEM morphology of the surface of residues from (1) PVA/APP20, (2) PVA/APP19/SP1, (3) PVA/APP17/SP3, (4) PVA/APP15/SP5 coatings.

The surface morphology of PVA/APP20 was inhomogeneous with a succession of layers. The char layer of PVA/APP19/SP1 presents several holes on the surface which suggests a poor cohesion of the residue, whereas, the residues of PVA/APP17/SP3 and PVA/APP15/SP5 appear more compact and homogeneous. Duquesne et al. [36] suspected that the addition of talc and APP in a PP matrix could result in the formation of magnesium phosphate and/or silico-phosphate structures which affected the mechanical properties of the char layer. Contrary to the results presented here, the layer formed could reduce the effectiveness of the flame-retardant system. Reaction between APP and sepiolite led to the formation of a silico-phosphate structure ($Si_xP_yO_z$) assumed to be responsible for the cohesion of the char layer. The incorporation of sepiolite promotes the development of a compact char layer which can limit the transfer of heat and flammable volatiles during combustion.

To verify this hypothesis, fire resistance tests were carried out on GFRP composite protected by PVA-based coatings using cone calorimeter.

3.5. Fire Resistance of GFRP Composite Laminate with PVA Coatings
3.5.1. Cone Calorimeter Tests

Figure 11 and Table 5 presents the evolution of the temperature at the backside of the samples based on the average between two tests. At 20 kW/m^2, temperature on the backside of GFRP composite laminate increased drastically to reach a steady state at 260 °C after 500 s. It can be observed that the addition of a PVA coating over the GFRP composite laminate significantly decreases the maximum temperature from 260 °C to 176 °C. The addition of 20 wt% of APP leads to the appearance of a temperature plateau between 250 and 750 s at 95 °C followed by an increase in temperature reaching

174 °C after 2000 s. For CP/PVA/APP17/SP3 sample, a first temperature plateau slightly shorter is also observed while the maximum temperature is slightly higher at 195 °C. On the contrary, CP/PVA/APP15/SP5 samples present a significantly longer plateau, from 250 to 850 s at 95 °C. In addition, the temperature reached by the sample after 2000 s is equivalent to CP/PVA and CP/PVA/APP20. The presence of a plateau at 100 °C has already been observed in the literature for intumescent coatings [37,38]. It was assumed that this phenomenon would be due to the swelling of the coating which would isolate the composite from the heat source. It can be hypothesized that this delay is due to the formation of an insulating layer which limits the diffusion of heat in the unexposed side of composite laminate. It should be noticed that CP/PVA sample does not show a plateau at 100 °C neither at 20 nor at 50 kW/m^2. For a 20 kW/m^2 heat flux the residue of the CP/PVA exhibits a cohesive intumescent layer; however, it is assumed that this char is less insulating.
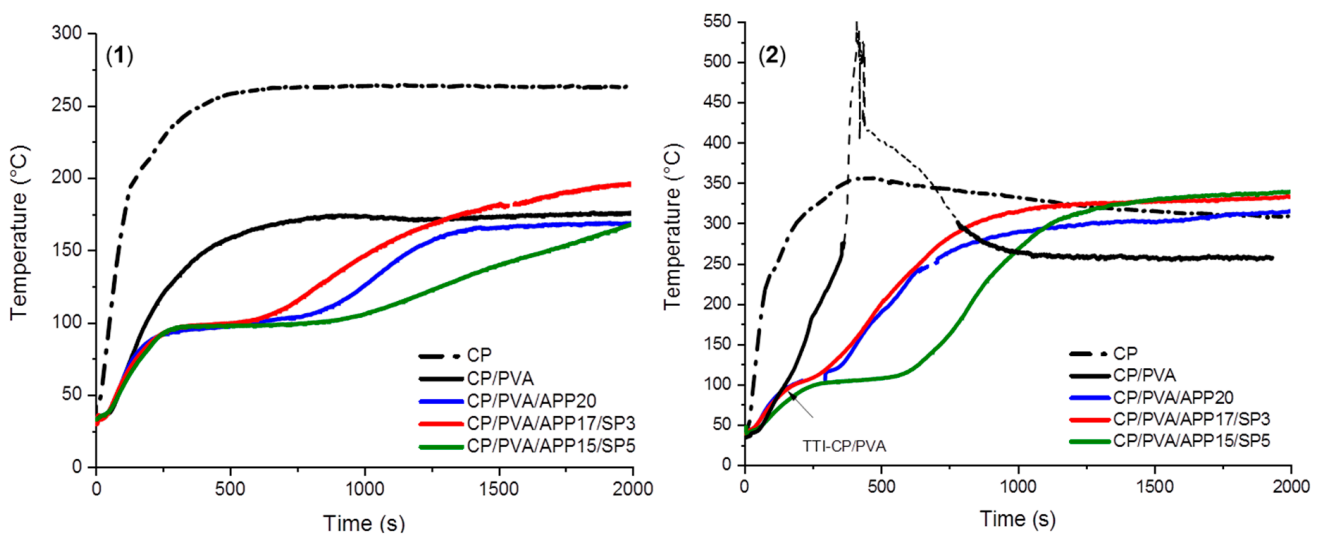

Figure 11. Temperature variation curve of the opposite fire-exposed face of the coating on GFRP composites laminates for a flux of 20 kW/m^2 (1) and 50 kW/m^2 (2).

Table 5. Temperature and time of ignition data for PVA-coated composite laminate submitted to 20 and 50 kW/m^2 fluxes.

Coated Composite Laminate (CP)	20 kW/m^2 flux		50 kW/m^2 flux			
	T_{MAX} (°C)	T_{END} (°C)	T_{MAX} (°C)	T_{END} (°C)	TTI (s)	TTF (s)
CP	263	263	353	301	-	-
CP/PVA	175	175	560	256	150	550
CP/PVA/APP20	168	168	329	298	1610	2050
CP/PVA/APP17/SP3	196	196	333	330	-	-
CP/PVA/APP15/SP5	169	169	345	330	-	-

The samples submitted to a 50 kW/m^2 heat flux exhibit similar behavior, with the exception of CP/PVA formulation. CP by itself exhibits a maximum temperature (350 °C) at 500 s and then reaches a plateau at circa 300 °C. CP/PVA attained the highest temperatures at 560 °C due to the self-ignition of the polymer after 150 s. High temperature rise (shown in dotted lines in Figure 11) between 360 s to 780 s is considered as a measurement artefact due to the presence of a flame on the unexposed face. Ignition of CP/PVA composites lead to the complete degradation of the resin matrix. The CP/PVA/APP20 samples ignited also after 1600 s, but the fire was limited to the PVA/APP coating and did not affect the back-temperature measurement.

It can be remarked that composite laminates protected by APP- or APP/SP-containing coatings exhibit a plateau at 100 °C, as it was observed at 20 kW/m^2. However, this

plateau is shorter. It can be noted that for the two fluxes, the plateau at 100 °C for the CP/PVA/APP15/SP5 is longer than that of CP/PVA/APP17/SP3 and CP/PVA/APP20. The temperatures reached by the CP/PVA/APP17/SP3 and CP/PVA/APP15/SP5 plates for a flux of 50 kW/m^2 were higher than CP/PVA/APP20, but they did not undergo self-ignition, which indicates a higher thermal stability due to an efficient char layer. It appears that the incorporation of 5 wt% of sepiolite gives rise to a threshold effect resulting in an improvement in the thermal barrier effect of the coating.

3.5.2. Characterization of Residues

In order to explain the presence of a threshold, DRX and SEM analyses of the residues obtained after the fire resistance tests were carried out.

SEM Analysis

EDX analysis was realized on residues after fire resistance tests and compared to the results obtained after fire reaction tests (Table 4). The compositions were obtained therefore either by direct analysis of the surface residue, or after grinding the residue with a test cone calorimeter at 50 kW/m^2.

Comparison between Tables 4 and 6 shows that the atomic compositions between the PVA/APP20 residues obtained after the cone tests in reaction and in fire resistance are similar. However, contrary to Table 4, the proportion of carbon did not increase between the formulations SP3 and SP5. The percentage of phosphorus is equivalent between the bulk and the surface of the residue; this highlights the homogeneity of the residue composition during the formation of the intumescent layer. The presence of nitrogen in the residue indicates a change in the degradation of the coating in the absence of flame. It can be concluded that part of ammonia in APP remained in the condensed phase.

Table 6. Quantitative analysis by SEM of surface of residues (a) and residues crushed (b) of coatings on composite laminate after cone calorimeter testing at 50 kW/m^2.

(a)							
Composition	%C	%O	%P	%Si	%Mg	%Na	%N
CP/PVA/APP20	14.7	53.1	29	-	-	2.7	Not detected
CP/PVA/APP17/SP3	39.2	35.9	14.7	2.6	1.4	1.1	5
CP/PVA/APP15/SP5	24.4	42.6	16.6	9.1	2.6	1.4	3
(b)							
Composition	%C	%O	%P	%Si	%Mg	%Na	%N
CP/PVA/APP20	31.2	44.6	21.4	-	-	1.43	Not detected
CP/PVA/APP17/SP3	39	36.9	16.7	3.2	0.93	0.83	2
CP/PVA/APP15/SP5	31.8	43.6	16.4	4.2	2.33	1.35	Not detected

XRD Analysis

The XRD patterns (Figure 12) of residues from PVA/APP/SP-coated composites laminates exposed to heat fluxes of 20 and 50 kW/m^2 show the presence of several crystalline phases. For a heat flux of 20 kW/m^2, $(NH_4)H_2PO_4$ was identified for the three compositions through the main peaks ($2\theta = 16.7°$, $23.7°$ and $29.0°$). Sepiolite ($2\theta = 7.3°$) and $(NH_4)_2MgH_4(P_2O_7),2H_2O$ ($2\theta = 16.0°$, $18.5°$ and $24.5°$) crystalline phases were observed for the PVA/APP17/SP3- and PVA/APP15/SP5-coated composites. Under these heating conditions, APP decomposes to create a phosphoric acid salt ($(NH_4)H_2PO_4$) which further reacts with sepiolite to form the crystalline phase $(NH_4)_2MgH_4(P_2O_7)_2H_2O$. In addition, the presence of sepiolite in XRD patterns suggests that part of sepiolite did not react at the temperature reached in these heating conditions. The presence of sepiolite in the residue could play a role in the structuration of the protective layer causing a limitation of the heat transfer from the coating to the GFRP composite laminate.
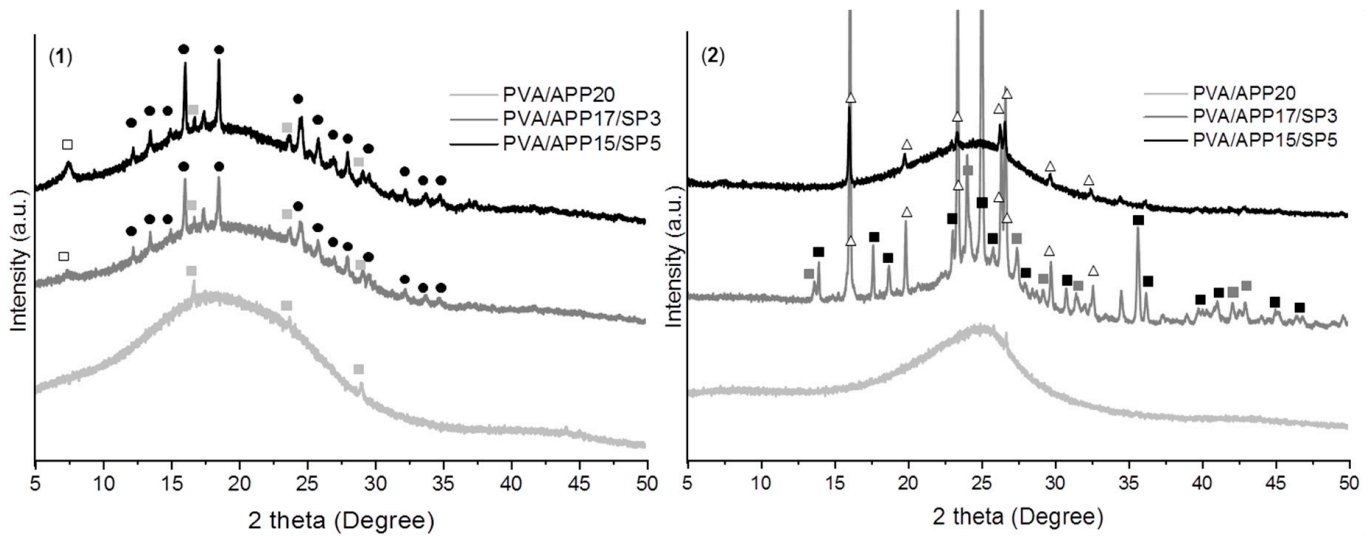
Figure 12. XRD patterns of PVA/APP20, PVA/APP17/SP3 and PVA/APP15/SP5 after fire resistance on cone calorimeter testing at (1) 20 kW/m^2 and (2) 50 kW/m^2 (($\square$): sepiolite, ($\blacksquare$): NaMg(PO$_3$)$_3$, ($\blacksquare$): SiP$_2$O$_7$, ($\blacksquare$): (NH$_4$)H$_2$PO$_4$, ($\bullet$): (NH$_4$)$_2$MgH$_4$(P$_2$O$_7$),2H$_2$O, ($\triangle$): Si$_x$P$_y$O$_z$).

For 50 kW/m^2 heat flux, CP/PVA/APP20 residue exhibits mainly an amorphous structure as proved by the large bump centered around 17°. Additionally, some undefined peaks (2θ = 25.8° and 26.7°) were also observed. For the CP/PVA/APP17/SP3 residue, NaMg(PO$_3$)$_3$ (with main peaks: 2θ = 23.4° and 25.0°), SiP$_2$O$_7$ (2θ = 24.0° and 26.3°) and Si$_x$P$_y$O$_z$ (2θ = 16.0° and 19.3°) crystalline phases were identified whereas, for the CP/PVA/APP15/SP5 residue, only the crystalline phase Si$_x$P$_y$O$_z$ was detected. XRD patterns of CP/PVA/APP17/SP3 and CP/PVA/APP15/SP5 are comparable to the spectra obtained on the residue after the cone calorimeter test of coating samples (Figure 7). The pattern is better defined in the case of the 3 wt% sepiolite-containing composition.

Comparison between residues from CP/PVA/APP/SP and PVA/APP/SP after oven conditioning in Figure 7 shows the formation of the same crystalline phases (NaMg(PO$_3$)$_3$, SiP$_2$O$_7$ and Si$_x$P$_y$O$_z$). This result means that coating during the fire resistance test would reach at least a temperature of 550 °C. The absence of crystalline phases NaMg(PO$_3$)$_3$ and SiP$_2$O$_7$ in the residue of PVA/APP/SP after fire reaction (Figure 6) would be due to the presence of the flame modifying the surface temperature of the coating.

Char Volume of Residues

Photogrammetry was performed on the residues after the cone calorimeter test to estimate the influence of APP and sepiolite on the coating intumescence. The residues obtained at 20 kW/m^2 are shown in Figure 13 and data are presented in Table 7. CP/PVA residue exhibits a large volume expansion, even though no intumescent flame retardant was added, resulting in a final volume of 117 cm^3. Swelling of PVA would be due to an appropriate viscosity of the molten polymer associated with the release of combustible gas causing the intumescence of the layer.
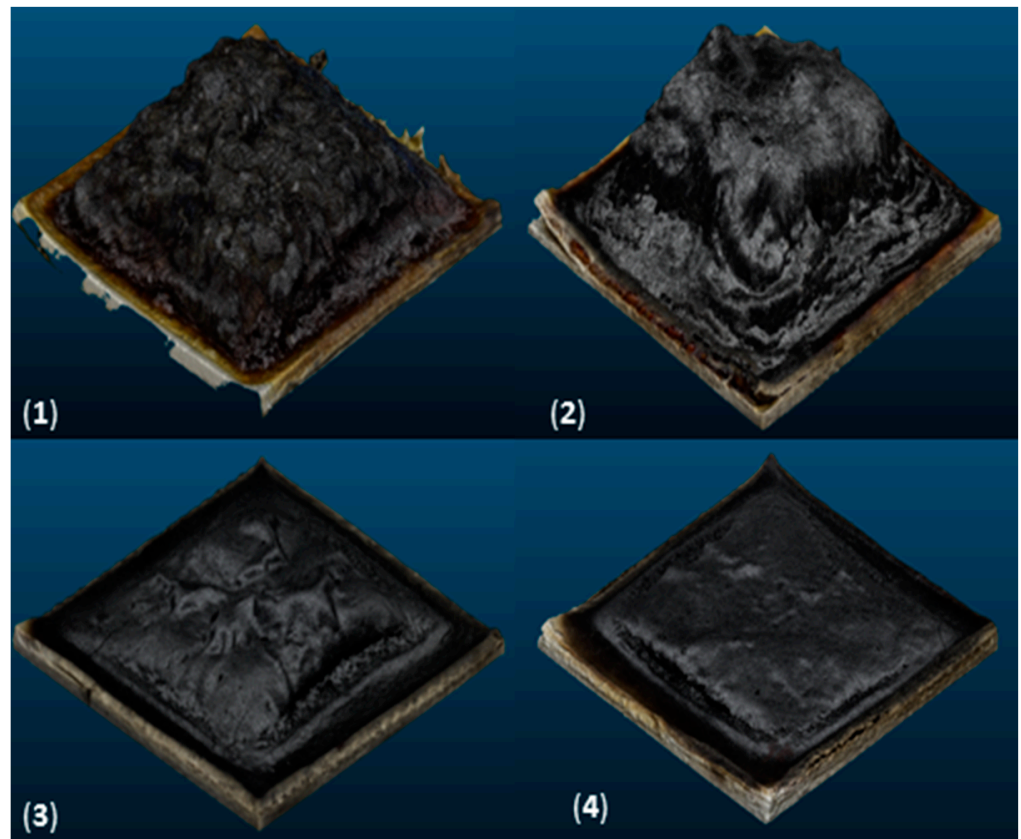
Figure 13. Photogrammetry of residues after fire resistance test at 20 kW/m^2 obtained by scatter plot for (1) PVA, (2) PVA/APP20, (3) PVA/APP17/SP3, (4) PVA/APP15/SP5.

Table 7. Residue volume of PVA-coated composite laminate after cone test at 20 kW/m^2 using scatter plot reconstruction with Agisoft Metashape software.

Coating Formulation	Volume (cm^3)
CP/PVA	117
CP/PVA/APP20	100 $\pm$ 7
CP/PVA/APP17/SP3	55 $\pm$ 4
CP/PVA/APP15/SP5	30 $\pm$ 8

CP/PVA/APP20 residue presents a volume of 100 $\pm$ 7 cm^3; the residue layer was thin in comparison to those of sepiolite containing coatings. The addition of 3 wt% and 5 wt% of sepiolite results in a decrease of expansion with volumes of respectively 55 $\pm$ 4 and 30 $\pm$ 8 cm^3.

The results indicate that the addition of sepiolite to the coating leads to the formation of a thick and compact layer, exhibiting a poor expansion.

The same trend was observed for the CP/PVA/APP/SP residues obtained after tests at a 50 kW/m^2 heat flux. The residues are presented in Figure 14; the volume of residues could not be assessed by photogrammetry due to a too-poor swelling.
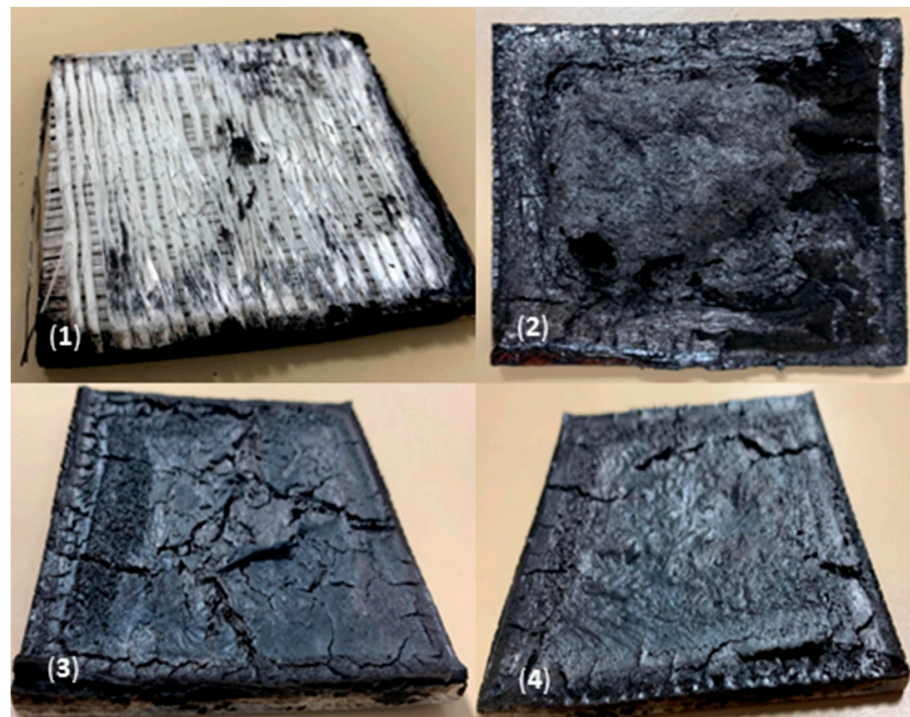
Figure 14. Photographs of char residues on glass-fiber-reinforced polymer (GFRP) composites after cone calorimeter experiments at 50 kW/m^2: (1) CP/PVA, (2) CP/PVA/APP20, (3) CP/PVA/APP17/SP3, (4) CP/PVA/APP15/SP5.

As indicated above, the PVA-coated composite laminate ignited causing the complete burning of the coating and then of the resin of the composite, leaving only the glass fibers after the test. As was observed on Figure 9, the residue of CP/PVA/APP exhibits a low swelling during reaction to fire tests. Moreover, the residue presents a fragile character and is not very cohesive as demonstrated by the SEM observations in Figure 10. The use of the PVA/APP17/SP3 and PVA/APP15/SP5 coatings resulted in the formation of a cohesive char, slightly swollen, exhibiting cracks which formed during cooling of the plates after testing. Those char layers constitute a protection for the composite resin.

The efficiency of APP/SP-containing coating as a thermal shield was assigned to the reactivity between APP and SP that leads to the formation of crystalline silicophosphate species as demonstrated by XRD. These phases impart cohesion to the layer limiting its swelling but emphasizing its protective feature. Due its high thermal stability, the formed inorganic layer is likely to reach a higher temperature and thus the heat loss by re-radiation will be higher according to the Stefan law. Re-radiation of a hot surface has already been demonstrated experimentally by Wu and al. [39] for polymer-nanocomposites-based thermosets that exhibit few or no charring. Hence storage and re-radiation by the layer delays heat transfer to the backside thus delaying and slowing down the temperature rise. Additionally, unreacted SP nanoparticles may also participate to the thermal barrier limiting heat transmission by accumulation at the surface [19].

4. Conclusions

In this study, a surface coating based on PVA containing APP and sepiolite was designed for protecting GFRP composite laminates. The deposition of a flame-retardant PVA suspension onto a glass fiber membrane enabled to prepare a fabric-based coating that exhibited further a good cohesion with the composite laminate. The fire behavior of coatings showed an increase of time to ignition and a drastic decrease of pHRR for coatings containing sepiolite. An optimum of performance for all fire reaction parameters has been demonstrated for 3 wt% of sepiolite with a reduction of pHRR by 70%, THR by

37% and an increase of TTI up to 65 s compared to PVA matrix in cone calorimeter tests. Despite a loss of thermal stability in TGA with a decrease of Tonset from 291 °C to 243 °C, PVA/APP17/SP3 showed the formation of the greater residue yield of circa 28 wt% at 700 °C. Moreover, a sepiolite–APP interaction in the condensed phase was evidenced leading to the formation of a crystalline phase in the residue which could not be identified. This $Si_xP_yO_z$ phase was highlighted in the residues of cone calorimeter tests regardless of the presence of a flame. A cohesive residue layer was formed during combustion reinforced by the inorganic crystalline phase. Once deposited on composite laminates, the APP/SP coatings enable an increase of the fire resistance evidenced by a delay and a slowdown of the backside temperature rise. PVA/APP15/SP5 is the most performant coating which enables to postpone the backside heating by respectively 1250 and 2000 s for a 20 and 50 kW/m^2 heat flux exposure. The increase of sepiolite content in the coating increases the thermal barrier effect by greatly delaying the backside temperature rise of the composite laminate. The shielding effect has been attributed to a re-radiation mechanism of the surface due to sepiolite. Combination of APP and sepiolite in PVA coating showed good efficiency to protect resin composite laminate.

Supplementary Materials: The following are available online at https://www.mdpi.com/2504-477 X/5/1/6/s1, Figure S1: Cross-section picture of composite coated by PVA/APP17/SP3.

Author Contributions: Conceptualization, L.F. (Léa Floch) and B.D.C.C.; methodology, L.F. (Léa Floch) and B.D.C.C.; software, B.D.C.C.; validation, L.F. (Léa Floch), B.D.C.C., L.F. (Laurent Ferry), D.P. and P.I.; formal analysis, L.F. (Léa Floch) and B.D.C.C.; investigation, L.F. (Léa Floch) and B.D.C.C.; data curation, L.F. (Léa Floch) and B.D.C.C.; writing—original draft preparation, L.F. (Léa Floch) and B.D.C.C.; writing—review and editing, L.F. (Léa Floch), L.F. (Laurent Ferry), D.P. and P.I.; supervision, L.F. (Laurent Ferry), D.P. and P.I.; project administration, L.F. (Laurent Ferry), D.P. and P.I. All authors have read and agreed to the published version of the manuscript.

Institutional Review Board Statement: Not applicable.

Informed Consent Statement: Not applicable.

Data Availability Statement: All data are described in this study and in the supplementary materials.

Conflicts of Interest: The authors declare no conflict of interest.

References

1. Tran, P.; Nguyen, Q.T.; Lau, K.T. Fire Performance of Polymer-Based Composites for Maritime Infrastructure. *Compos. Part B* **2018**, *155*, 31–48. [CrossRef]
2. Mouritz, A.P.; Gellert, E.; Burchill, P.; Challis, K. Review of Advanced Composite Structures for Naval Ships and Submarines. *Compos. Struct.* **2001**, *53*, 21–41. [CrossRef]
3. Kandola, B.K.; Kandare, E. *Advances in Fire Retardant Materials: Composites Having Improved Fire Resistance*; Woodhead Publishing: Cambridge, UK, 2008. [CrossRef]
4. Kandola, B.K.; Ebdon, J.R.; Luangtriratana, P.; Krishnan, L. Novel Flame Retardant Thermoset Resin Blends Derived from a Free-Radically Cured Vinylbenzylated Phenolic Novolac and an Unsaturated Polyester for Marine Composites. *Polym. Degrad. Stab.* **2016**, *127*, 56–64. [CrossRef]
5. Kandare, E.; Chukwudolue, C.; Kandola, B.K. The Use of Fire-Retardant Intumescent Mats for Fire and Heat Protection of Glass Fibre-Reinforced Polyester Composites: Thermal Barrier Properties. *Fire Mater.* **2010**, *34*, 21–38. [CrossRef]
6. Tibiletti, L.; Longuet, C.; Ferry, L.; Coutelen, P.; Mas, A.; Robin, J.J.; Lopez-Cuesta, J.M. Thermal Degradation and Fire Behaviour of Unsaturated Polyesters Filled with Metallic Oxides. *Polym. Degrad. Stab.* **2011**, *96*, 67–75. [CrossRef]
7. Kandare, E.; Kandola, B.K.; Price, D.; Nazaré, S.; Horrocks, R.A. Study of the Thermal Decomposition of Flame-Retarded Unsaturated Polyester Resins by Thermogravimetric Analysis and Py-GC/MS. *Polym. Degrad. Stab.* **2008**, *93*, 1996–2006. [CrossRef]

8. Tibiletti, L.; Ferry, L.; Longuet, C.; Mas, A.; Robin, J.; Lopez-Cuesta, J.-M. Thermal Degradation and Fire Behavior of Thermoset Resins Modified with Phosphorus Containing Styrene. *Polym. Degrad. Stab.* **2012**, *97*, 2602–2610. [CrossRef]

9. Shekarchi, M.; Farahani, E.M.; Yekrangnia, M.; Ozbakkaloglu, T. Mechanical Strength of CFRP and GFRP Composites Filled with APP Fire Retardant Powder Exposed to Elevated Temperature. *Fire Saf. J.* **2020**, *115*, 15. [CrossRef]

10. Sorathia, U.; Gracik, T.; Ness, J.; Durkin, A.; Williams, F.; Hunstad, M.; Berry, F. Evaluation of Intumescent Coatings for Shipboard Fire Protection. *J. Fire Sci.* **2003**, *21*, 423–450. [CrossRef]

11. Luangtriratana, P.; Kandola, B.K.; Myler, P. Ceramic Particulate Thermal Barrier Surface Coatings for Glass Fibre-Reinforced Epoxy Composites. *Mater. Des.* **2014**, *68*, 232–244. [CrossRef]

12. Luangtriratana, P.; Kandola, B.K.; Duquesne, S.; Bourbigot, S. Quantification of Thermal Barrier Efficiency of Intumescent Coatings on Glass Fibre-Reinforced Epoxy Composites. *Coatings* **2018**, *8*, 347. [CrossRef]

13. Bourbigot, S.; Le Bras, M.; Duquesne, S.; Rochery, M. Recent Advances for Intumescent Polymers. *Macromol. Mater. Eng.* **2004**, *289*, 499–511. [CrossRef]

14. Alkan, M.; Benlikaya, R. Poly(Vinyl Alcohol) Nanocomposites with Sepiolite and Heat-Treated Sepiolites. *J. Appl. Polym. Sci.* **2009**, *112*, 3764–3774. [CrossRef]

15. Lin, J.S.; Liu, Y.; Wang, D.Y.; Qin, Q.; Wang, Y.Z. Poly(Vinyl Alcohol)/Ammonium Polyphosphate Systems Improved Simultaneously Both Fire Retardancy and Mechanical Properties by Montmorillonite. *Ind. Eng. Chem. Res.* **2011**, 9998–10005. [CrossRef]

16. Zhao, C.; Liu, Y.; Wang, D.; Wang, D.; Wang, Y. Synergistic Effect of Ammonium Polyphosphate and Layered Double Hydroxide on Flame Retardant Properties of Poly (Vinyl Alcohol). *Polym. Degrad. Stab.* **2008**, *93*, 1323–1331. [CrossRef]

17. Quach, Y.; Ferry, L.; Sonnier, R. Efficiency of Wollastonite and Ammonium Polyphosphate Combinations on Flame Retardancy of Polystyrene. *Polym. Adv. Technol.* **2012**, *10*, 104–113. [CrossRef]

18. Rimez, B.; Rahier, H.; Biesemans, M.; Bourbigot, S.; Van Mele, B. Flame Retardancy and Degradation Mechanism of Poly(Vinyl Acetate) in Combination with Intumescent Flame Retardants: I. Ammonium Poly(Phosphate). *Polym. Degrad. Stab.* **2015**, *121*, 321–330. [CrossRef]

19. Laoutid, F.; Bonnaud, L.; Alexandre, M.; Lopez-Cuesta, J.M.; Dubois, P. New Prospects in Flame Retardant Polymer Materials: From Fundamentals to Nanocomposites. *Mater. Sci. Eng. R Rep.* **2009**, *63*, 100–125. [CrossRef]

20. Hapuarachchi, T.D.; Peijs, T. Composites: Part A Multiwalled Carbon Nanotubes and Sepiolite Nanoclays as Flame Retardants for Polylactide and Its Natural Fibre Reinforced Composites. *Compos. Part A* **2010**, *41*, 954–963. [CrossRef]

21. Bodzay, B.; Bocz, K.; Bárkai, Z.; Marosi, G. Influence of Rheological Additives on Char Formation and Fire Resistance of Intumescent Coatings. *Polym. Degrad. Stab.* **2011**, *96*, 355–362. [CrossRef]

22. Tian, G.; Han, G.; Wang, F.; Liang, J. Sepiolite Nanomaterials: Structure, Properties and Functional Applications, Nanomateri. In *Nanomaterials from Clay Minerals*; Elsevier: Amsterdam, The Netherlands, 2019.

23. Huang, N.H.; Chen, Z.J.; Wang, J.Q.; Wei, P. Synergistic Effects of Sepiolite on Intumescent Flame Retardant Polypropylene. *Express Polym. Lett.* **2010**, *4*, 743–752. [CrossRef]

24. Vahabi, H.; Lin, Q.; Vagner, C.; Cochez, M.; Ferriol, M.; Laheurte, P. Investigation of Thermal Stability and Flammability of Poly(Methyl Methacrylate) Composites by Combination of APP with ZrO2, Sepiolite or MMT. *Polym. Degrad. Stab.* **2016**, *124*, 60–67. [CrossRef]

25. Pappalardo, S.; Russo, P.; Acierno, D.; Rabe, S.; Schartel, B. The Synergistic Effect of Organically Modified Sepiolite in Intumescent Flame Retardant Polypropylene. *Eur. Polym. J.* **2016**, *76*, 196–207. [CrossRef]

26. Carretier, V.; Delcroix, J.; Pucci, M.F.; Rublon, P. Influence of Sepiolite and Lignin as Potential Synergists on Flame Retardant Systems in Polylactide (PLA) and Polyurethane Elastomer (PUE). *Materials* **2020**, *13*, 2450. [CrossRef]

27. García-romero, E.; Suárez, M. Sepiolite–Palygorskite: Textural Study and Genetic Considerations. *Appl. Clay Sci.* **2013**, *86*, 129–144. [CrossRef]

28. Peng, S.; Zhou, M.; Liu, F.; Zhang, C. Flame-Retardant Polyvinyl Alcohol Membrane with High Transparency Based on a Reactive Phosphorus- Containing Compound. *R. Soc. Open Sci.* **2017**, *4*. [CrossRef]

29. Zhou, X.-Y.; Jia, D.-M.; Cui, Y.-F.; Xie, D. Kinetics Analysis of Thermal Degradation Reaction of PVA and PVA/Starch Blends. *Reinf. Plast. Compos.* **2009**, *28*, 2771–2780. [CrossRef]

30. Camino, G.; Costa, L.; Trossarelli, L.; Costanzi, F.; Pagliari, A. Study of the Mechanism of Intumescence in Fire Retardant Polymers: Part VI-Mechanism of Ester Formation in Ammonium Polyphosphate-Pentaerythritol Mixtures. *Polym. Degrad. Stab.* **1985**, *12*, 213–228. [CrossRef]

31. Camino, G.; Luda, M.P. Mechanistic Study of Intumescence. In *FRPM 97: 6th European Meeting on Fire Retardancy of Polymeric Materials*; Royal Society of Chemistry: London, UK, 1998. [CrossRef]

32. Zhang, Y.; Wang, L.; Wang, F.; Liang, J.; Ran, S. Phase Transformation and Morphology Evolution of Sepiolite Fibers during Thermal Treatment. *Appl. Clay Sci.* **2017**, *143*, 205–211. [CrossRef]

33. Winans, R.E.; Seifert, S.; Carrado, K.A. In Situ SAXS Studies of the Structural Changes of Sepiolite Clay and Sepiolite-Carbon Composites with Temperature. *Chem. Mater.* **2002**, *14*, 739–742. [CrossRef]

34. Schartel, B.; Hull, T.R. Development of Fire-Retarded Materials—Interpretation of Cone Calorimeter Data. *Fire Mater.* **2007**, *31*, 327–354. [CrossRef]

35. Dumazert, L.; Rasselet, D.; Lopez-Cuesta, J.-M.; Pang, B.; Gallard, B.; Kennouche, S. Thermal Stability and Fire Reaction of Poly (Butylene Succinate) Nanocomposites Using Natural Clays and FR Additives. *Polym. Adv. Technol.* **2018**, *29*, 69–83. [CrossRef]

36. Duquesne, S.; Samyn, F.; Bourbigot, S.; Amigouet, P.; Jouffret, F.; Shen, K. Influence of Talc on the Fire Retardant Properties of Highly Filled Intumescent Polypropylene Composites. *Polym. Adv. Technol.* **2008**, *19*, 620–627. [CrossRef]

37. Pötzsch, S.; Krüger, S.; Sklorz, C.; Borch, J.; Hilse, T.; Otremba, F. The Fire Resistance of Lightweight Composite Tanks Depending on Fire Protection Systems. *Fire Saf. J.* **2018**, *100*, 118–127. [CrossRef]

38. Geoffroy, L.; Samyn, F.; Jimenez, M.; Bourbigot, S. Intumescent Polymer Metal Laminates for Fire Protection. *Polymers* **2018**, *10*, 995. [CrossRef]

39. Wu, G.M.; Schartel, B.; Bahr, H.; Kleemeier, M.; Yu, D.; Hartwig, A. Experimental and Quantitative Assessment of Flame Retardancy by the Shielding Effect in Layered Silicate Epoxy Nanocomposites. *Combust. Flame* **2012**, *159*, 3616–3623. [CrossRef]